

Preparation of Aluminum-Containing Self-Standing Mesoporous Silica Films

Naoki Shimura[1] **and Makoto Ogawa***[,1,2]

[1]Graduate School of Science and Engineering, Waseda University, Nishiwaseda 1-6-1, Shinjuku-ku, Tokyo 169-8050

[2]Department of Earth Sciences, Waseda University, Nishiwaseda 1-6-1, Shinjuku-ku, Tokyo 169-8050

Received October 31, 2003; E-mail: makoto@waseda.jp

Siliceous and aluminum-containing self-standing mesoporous silica films with the thickness of ca. 50 μm were synthesized by the solvent evaporation method from tetramethoxysilane, aluminum chloride hexahydrate, and octadecyltrimethylammonium chloride. The films possessed highly ordered mesostructures and large surface areas (over ca. 700 $m^2 g^{-1}$). The mesostructures of the products were controlled by the chemical compositions (Si/surfactant); siliceous mesostructured materials with hexagonal (*P6m*) and cubic (*Pm3n*) phases were obtained when the molar Si/surfactant ratios were 9 and 8, respectively. The aluminum-containing films with the molar Si/Al ratios of 50, 20, and 10 were also synthesized.

Mesoporous silicas prepared by supramolecular templating method have been investigated from both fundamental and practical viewpoints because of their ordered pore arrangements, pore size uniformity, high porosity, large surface area, and possible surface engineering.[1–4] Morphology of the mesoporous silicas is an important issue for their practical applications as well as for elucidation of their formation mechanisms.[5] Film is an attractive morphology for such uses as separation, sensor, and coating, to which powder samples do not have an access. Accordingly, the syntheses of mesoporous silica films with various thicknesses and chemical compositions have been reported[6] after our successful preparation of the coating films by the solvent evaporation method.[7,8]

The solvent evaporation method, in which soluble silica oligomers and surfactants cooperatively assemble to form highly ordered mesostructures during solvent evaporation from homogeneous solution, was developed for the preparation of mesoporous silica films.[7,8] Due to the ease of synthetic operation and the quality of the resulting materials, the solvent evaporation method became a versatile technique to fabricate mesoporous silicas in such morphology as coating films,[7–12] self-standing films,[13–16] fibers,[17] and hollow spheres.[18] In order to vary mesostructures, quaternary ammonium surfactants[7–18] and triblock-copolymers[19–21] have been used as the supramolecular templates.

This paper reports the preparation of self-standing mesoporous silica (both siliceous and aluminum-containing) films with highly ordered mesostructures. There are few reports on the preparation of self-standing porous silica films with surfactant templates.[13–16] When the solvent evaporation method is used, rapid solvent evaporation before the gelation is a crucial factor to obtain highly ordered mesostructures.[7–21] We have prepared self-standing porous silica films with the thickness of ca. 50 μm by the copolymerization of trimethoxyvinylsilane (abbreviated as TMVS) and tetramethoxysilane in the presence of alkyltrimethylammonium chlorides. The added TMVS played an important role in suppressing the rapid gelation.[13] In the present study, we optimized conditions (solvent and humidity) to synthesize self-standing mesoporous silica films without using TMVS. The effects of the humidity and of the Si/surfactant ratios of the starting solutions on the mesostructures were also investigated.

The introduction of heteroelements such as aluminum[22–28] and titanium[29–36] into mesoporous silicas is a way to modify their surface properties. We have reported titanium-containing self-standing mesoporous silica films and their photocatalytic abilities for the reduction of carbon dioxides to methane and methanol.[15,16] We have also reported the synthesis of the aluminum-containing mesoporous silica coating films with the thickness of several hundreds of nm.[37,38] The acidity of the films was evaluated by the adsorptive properties for a cationic azobenzene derivative, *p*-(ω-dimethyl-hydroxyethylammonioethoxy)-azobenzene bromide,[37,38] since bulk characterization techniques for acidity including solid-state NMR and temperature programmed desorption of basic molecules are difficult to apply for such thin coating films. The preparation of the aluminum-containing self-standing mesoporous silica films is worth investigating to overcome this limitation. The states of the introduced aluminum as well as the mesostructures of the films were investigated when the molar Si/Al ratios were 50, 20, and 10.

Experimental

Materials. Tetramethoxysilane (abbreviated as TMOS) and octadecyltrimethylammonium chloride (abbreviated as C18TAC) were obtained from Tokyo Kasei Kogyo Co., Ltd. and were used without further purification. Aluminum chloride hexahydrate (abbreviated as $AlCl_3 \cdot 6H_2O$) was obtained from Kanto Chemical Co., Inc. and was used as received. Methanol and hydrochloric acid were reagent grade, obtained from Kanto Chemical Co., Inc.

Sample Preparation. A typical synthetic procedure for the siliceous self-standing silica films is shown below. TMOS (1.00

Published on the web August 6, 2004; DOI 10.1246/bcsj.77.1599

g), deionized water (0.236 g), and 0.1 M HCl aqueous solution (0.050 g) were mixed for 30 min at 273 K with magnetic stirring. To which solution was added methanol (0.50 g), C18TAC (0.208, 0.229, 0.254 or 0.286 g), and 1.0 M HCl aqueous solution (0.050 g), and each mixture was allowed to react for 15 min at 273 K. Then the resulting solution was deposited on a poly(ethylene) film (casting area of ca. 80 cm^2) under controlled humidity. The humidity was adjusted in a closed glove bag between 65 and 75% at ambient temperature. The film (Si/C18TAC = 9) was also prepared in a similar way where methanol (0.50 g) was not added. In order to investigate the effects of the humidity on the mesostructures, we also examined the preparations of the films under various humidity values: 30, 35, 40, 45, 50, 55, 60, 65, 70, and 75%. The films were dried at ambient temperature under humidity less than 50% for 1 day to remove the solvents and to promote the condensation. The dried films were peeled off from the substrate to obtain self-standing silica-surfactant films. In order to remove surfactants, the as-synthesized films were calcined in air at 823 K for 10 h at a heating rate of 150 $K\,h^{-1}$. The molar ratios of TMOS:deionized water: HCl:C18TAC were 1:2.81:0.008:1/11, 1/10, 1/9, and 1/8.

Aluminum-containing self-standing silica-surfactant films were prepared in a way similar to that for the preparation of the siliceous self-standing silica films described before. A typical synthetic procedure for the aluminum-containing self-standing silica films prepared at the molar Si/Al ratios of 50 and 20 is shown below. $AlCl_3 \cdot 6H_2O$ (0.032, 0.080, and 0.160 g), TMOS (1.00 g), deionized water (0.236 g), and 0.1 M HCl aqueous solution (0.050 g) were mixed for 60 min at 273 K with magnetic stirring. To which solution was added C18TAC (0.229 g) and 1.0 M HCl aqueous solution (0.050 g), and each mixture was allowed to react for another 15 min at 273 K. The film (Si/Al = 50) was also prepared in a similar way where methanol (0.50 g) was added with C18TAC. In the case of the aluminum-containing films prepared at the molar Si/Al ratio of 50, the molar TMOS/C18TAC ratios of 9 and 11 (weight of C18TAC was 0.208 and 0.254 g, respectively) were also examined. A typical synthetic procedure for the film prepared at Si/Al = 10 was different from that for the films prepared at Si/Al = 50 and 20, as shown below. TMOS (1.00 g), C18TAC (0.229 g), deionized water (0.236 g), and 0.1 M HCl aqueous solution (0.050 g) were mixed for 10 min at 273 K with magnetic stirring. $AlCl_3 \cdot 6H_2O$ (0.160 g) and 1.0 M HCl aqueous solution (0.050 g) were added to the mixture and this mixture was allowed to react for another 20 min at 273 K. The resulting solution was deposited on a poly(ethylene) film by the same procedure as employed for the siliceous self-standing silica films. The molar ratios of TMOS:$AlCl_3 \cdot 6H_2O$:deionized water:HCl:C18TAC were 1:1/50, 1/20, and 1/10:2.81:0.008:1/10.

Characterization. X-ray diffraction (XRD) was performed on a RAD IB diffractometer (Rigaku) using monochromatic Cu Kα radiation, operated at 40 kV and 20 mA. Scanning electron micrographs (SEM) were obtained on a Hitachi S-2380N scanning electron microscope. The nitrogen adsorption/desorption isotherms of the calcined films were measured at 77 K on a Belsorp 28SA instrument (Bel Japan Inc.). The sample was cut in small pieces (less than 5 mm) to put into the sample holder. Prior to the measurements, the sample was dried at 393 K under vacuum for 3 h. Solid-state ^{27}Al nuclear magnetic resonance (NMR) spectra were recorded on a JEOL CMX400 spectrometer at 104.17 MHz with magic angle spinning.

Results

Siliceous Films. Self-standing films with the lateral size of a few cm were obtained irrespective of the Si/C18TAC ratios. The films were highly transparent and continuous. SEM observations indicated that the surfaces of the films were smooth. The SEM image of the surface for the calcined film prepared at Si/C18TAC = 9 is shown in Fig. 1 as an example. The film thickness was determined from the cross-sectional view of the films to be ca. 50 μm. The film thickness can be varied to some extent depending on the conditions such as the amount of methanol added and the viscosity of the solutions. The films should be thicker than ca. 10 μm, since thinner films were broken into small pieces when peeled off from the poly(ethylene) substrate.

The morphology did not change upon the surfactant removal by the calcination. When the surfactant was extracted with 1.0 M HCl ethanol solution, the film cracked significantly. When the films were synthesized from TMOS, C18TAC, and HCl aqueous solutions, the films were cracked (below 30 mm^2)

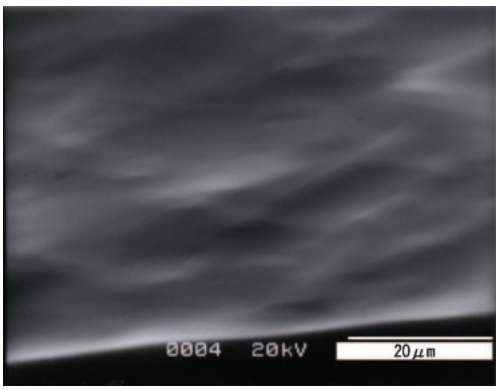

Fig. 1. SEM image of the surface for the siliceous film (Si/C18TAC = 9) after the calcination.

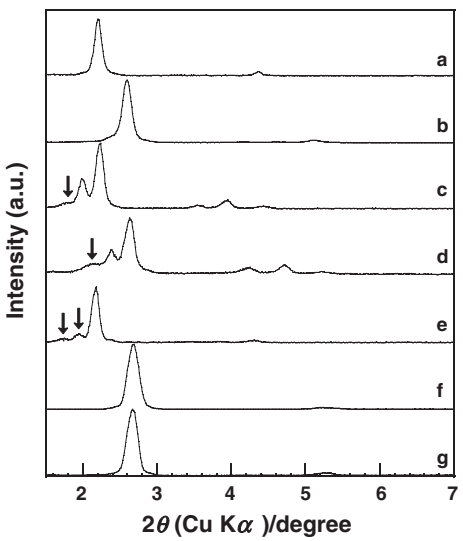

Fig. 2. X-ray diffraction patterns of the siliceous self-standing films (a) as-synthesized film (Si/C18TAC = 9) at the surface, (b) calcined film (Si/C18TAC = 9) at the surface, (c) as-synthesized film (Si/C18TAC = 8) at the surface, (d) calcined film (Si/C18TAC = 8) at the surface, (e) as-synthesized film (Si/C18TAC = 9) prepared under humidity of 50% at the surface, (f) calcined film (Si/C18TAC = 9) at the substrate side, and (g) calcined film (Si/C18TAC = 8) at the substrate side.

Table 1. Assignments and *d* Values of the Siliceous Self-Standing Silica Films

Si/C18TAC	As-synthesized film		Calcined film	
	d value/nm	Assignment	*d* value/nm	Assignment
8 (Film surface)	4.9, 4.4, 4.0	(200), (210), (211)	4.1, 3.7, 3.4	(200), (210), (211)
9 (Film surface)	4.0	(100)	3.4	(100)
8 (Substrate side)	3.8	(100)	3.3	(100)
9 (Substrate side)	3.9	(100)	3.3	(100)

during the calcination.

The effects of the Si/surfactant ratios on the mesostructures of the mesoporous silica coating films were reported.[39] The molar Si/C18TAC ratios of the starting solutions were varied, in order to vary the mesostructures of the present self-standing films. Sharp diffraction peaks were observed at lower 2θ regions in the XRD patterns of all the as-synthesized films, indicating that the films possessed ordered mesostructures. The XRD patterns of the films prepared at Si/C18TAC = 8 and 9 are shown in Fig. 2. The *d* values that correspond to the distances between adjacent pores are summarized in Table 1. The XRD pattern of the film prepared at Si/C18TAC = 8 (Fig. 2c) was attributed to a cubic (*Pm*3*n*) mesostructure (4.9 nm: (200), 4.4 nm: (210), and 4.0 nm: (211)). The XRD pattern of the film prepared at Si/C18TAC = 9 (Fig. 2a) showed a single peak ($d = 4.0$ nm). The XRD pattern of the grinded film prepared at Si/C18TAC = 9 showed peaks (4.0 nm: (100), 2.3 nm: (110), and 1.5 nm: (210)) ascribable to a hexagonal (*P*6*m*) mesostructure. Thus, reflections ascribable to (110) and (210) were absent in the XRD pattern at the surface of the film prepared at Si/C18TAC = 9 (Fig. 2a), indicating that the film was composed of cylindrical surfactant aggregates oriented parallel to the film plane as reported for the coating films.[39] The films prepared at Si/C18TAC = 10 and 11 also possessed hexagonal (*P*6*m*) mesostructures (4.0 and 3.9 nm for (100) reflection of the films prepared at Si/C18TAC = 10 and 11, respectively). Thus, the mesostructures of the siliceous films were controlled by varying the molar Si/surfactant ratios of the precursor solutions.

The reaction (Si/C18TAC = 9) was conducted several times to check the reproducibility of the results. Self-standing silica-C18TAC films with hexagonal mesostructures were obtained in all the trials, the *d* (100) values of the as-synthesized films varied over the range of 3.9–4.5 nm.

Humidity when the precursor solution was deposited on the poly(ethylene) substrate is another factor to determine the mesostructures of the films. The XRD patterns of the as-synthesized films prepared under the humidity values of 50 and 65% are shown in Figs. 2e and 2a as examples. The films prepared under the humidity of less than ca. 50% had cubic (*Pm*3*n*) mesostructures, while the films prepared under the humidity values over ca. 55% possessed hexagonal (*P*6*m*) mesostructures.

Sharp diffraction peaks were observed at lower 2θ regions in the XRD patterns of all the calcined films as shown in Figs. 2b, 2d, 2f, and 2g, indicating that the ordered mesostructures were retained after the surfactant removal. The *d* values of the calcined films are also summarized in Table 1. The *d* values decreased upon the surfactant removal, indicating the condensation of remaining silanol groups in the silica walls during the calcination.

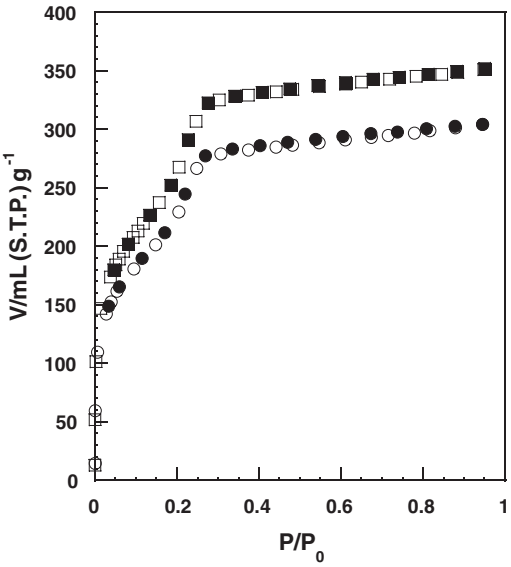

Fig. 3. Nitrogen adsorption/desorption isotherms of the siliceous self-standing silica films prepared at Si/C18TAC = 9 (adsorption: open circle, desorption: filled circle) and 8 (adsorption: open square, desorption: filled square).

In the case of coating films on glass substrate, the regularity of pore arrangement at the substrate was reported to be different from that at the film surface.[40] The XRD pattern at the substrate side of the film prepared at Si/C18TAC = 8 was attributed to a hexagonal (*P*6*m*) mesostructure (Fig. 2g), while that obtained for the film surface was ascribed to a cubic mesostructure (Fig. 2d). The heterogeneity of the mesostructures was thought to be caused by the heterogeneity of the solvent evaporation. The films prepared at Si/C18TAC = 9, 10, and 11 possessed hexagonal (*P*6*m*) mesostructures at the surface and the substrate side, while the *d* values at the substrate side were different from those at the film surface, as shown in Figs. 2b and 2f for the XRD patterns of the calcined film prepared at Si/C18TAC = 9.

Nitrogen adsorption/desorption isotherms of the calcined siliceous films prepared at Si/C18TAC = 8 and 9 are shown in Fig. 3. The nitrogen adsorption isotherms of the films followed type IV, showing that the films were mesoporous. The Brunauer–Emmett–Teller (BET) surface areas[41] of the films prepared at Si/C18TAC = 8 and 9 were determined from the adsorption isotherms to be 880 and 780 $m^2\,g^{-1}$, respectively. The average pore diameters were derived from the adsorption isotherms by Barrett–Joyner–Halenda (BJH) plots[42] to be 2.5 nm irrespective of the Si/C18TAC ratios.

Aluminum-Containing Films. Si/Al = 50: Irrespective of the Si/C18TAC ratios, highly transparent and continuous self-standing films with the thickness of ca. 50 μm and the lateral size of a few cm were obtained. The morphology did not change upon the surfactant removal. A photograph of the calcined film prepared at the molar Si/C18TAC ratio of 10 is shown in Fig. 4a.

The XRD patterns at the surfaces of the films prepared at Si/C18TAC = 10 and Si/Al = 50, 20, and 10 are shown in Fig. 5, and the *d* values of these films are summarized in Table 2. The molar Si/C18TAC ratios in the starting solutions were varied in order to control the mesostructures. The XRD pattern at the surface of the as-synthesized film prepared at Si/C18TAC = 9 showed three diffraction peaks ascribable to a cubic (*Pm*3*n*) mesostructure (5.1 nm: (200), 4.7 nm: (210), and 4.2 nm: (211)) (Fig. 5g). The surfaces of the as-synthesized films prepared at Si/C18TAC = 10 (Fig. 5a shows the XRD pattern) and 11 had hexagonal (*P*6*m*) mesostructures with the *d* (100) values of 4.5 and 4.0 nm, respectively. Thus, the mesostructures at the surface of the films prepared at Si/Al = 50 were controlled by varying the Si/C18TAC ratios of the starting solutions, as observed for the siliceous films. The XRD pattern at the surface of the calcined film prepared at Si/C18TAC = 10 is shown in Fig. 5b. The ordered mesostructures were retained after the surfactant removal, and the *d* values decreased upon the surfactant removal (Table 2), as pointed out for the siliceous films. The XRD patterns at the substrate side of the as-synthesized films prepared at Si/C18TAC = 9, 10, and 11 showed broad peaks, while those films at the film surface had ordered mesostructures. When the films were synthesized from TMOS, $AlCl_3 \cdot 6H_2O$, C18TAC, methanol, and HCl aqueous solutions, the XRD patterns at the surface of the as-synthesized films were broad.

Figure 6a shows the nitrogen adsorption/desorption isotherms obtained for the aluminum-containing film prepared at Si/C18TAC = 10. The adsorption isotherm followed type IV, showing that the film was mesoporous. The surface area and the average pore diameter were derived from the adsorption isotherm by BET[41] and BJH[42] plots to be 870 $m^2 g^{-1}$ and 2.6 nm, respectively.

We have already reported the preparation of the aluminum-containing mesoporous silica coating films.[37,38] The thickness of the films on glass substrate should be less than 1 μm in order to stick the film to the substrate. Bulk characterizations such as NMR and TPD have been difficult to apply for such thin coating films. On the other hand, self-standing films with quantity (ca. several hundred of mg) large enough for such experiments are

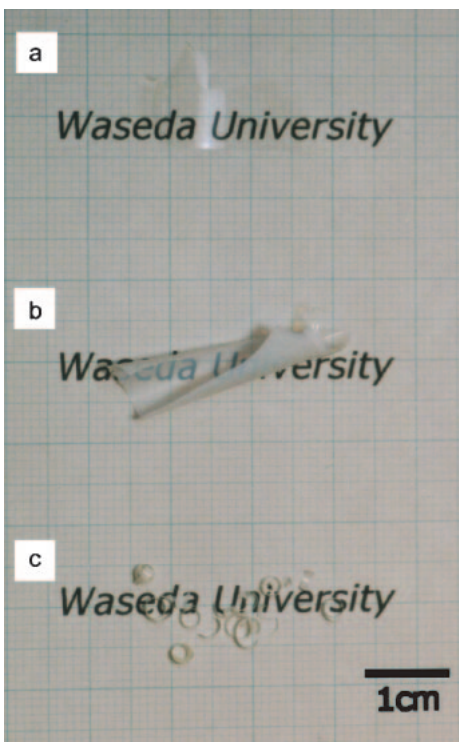

Fig. 4. The photograph of the aluminum-containing self-standing silica films prepared at Si/Al = (a) 50, (b) 20, and (c) 10 after the calcination.

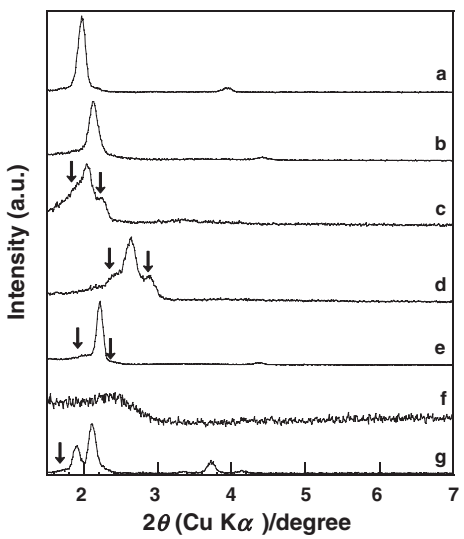

Fig. 5. X-ray diffraction patterns of the aluminum-containing self-standing silica films prepared at the Si/C18TAC ratio of 10 at the surface (a) as-synthesized film (Si/Al = 50), (b) calcined film (Si/Al = 50), (c) as-synthesized film (Si/Al = 20), (d) calcined film (Si/Al = 20), (e) as-synthesized film (Si/Al = 10), (f) calcined film (Si/Al = 10), and (g) as-synthesized film (Si/Al = 50, Si/C18TAC = 9).

Table 2. Assignments and *d* Values of the Aluminum-Containing Self-Standing Silica Films at the Surface

Si/Al	As-synthesized film		Calcined film	
	d value/nm	Assignment	*d* value/nm	Assignment
50	4.5	(100)	4.2	(100)
20	4.8, 4.4, 4.0	(200), (210), (211)	3.7, 3.3, 3.1	(200), (210), (211)
10	4.6, 4.1, 3.8	(200), (210), (211)	3.7	—

easily obtained in the present synthesis.

The ^{27}Al MAS NMR spectra of the films prepared at Si/Al = 50 showed two signals, at 53 and 0 ppm, attributable to tetrahedrally and octahedrally coordinated aluminums, respectively (Figs. 7a and 7b for the films prepared at Si/C18TAC = 10). The relative contribution of the signals at 53 ppm to those at 0 ppm was ca. 10%, indicating that the most of the aluminum in the as-synthesized film was present as octahedrally coordinated species. The relative contribution of the signals at 53 ppm to those at 0 ppm dramatically increased to ca. 85% from ca. 10% by the calcination.

Si/Al = 20 and 10: The as-synthesized self-standing films with the thickness of ca. 50 μm and the lateral size of a few cm were also obtained when the molar Si/Al ratios were 20 and 10. The as-synthesized and the calcined films were cloudy (Figs. 4b and 4c show the photographs of the calcined films), while the siliceous and the low aluminum content (Si/Al = 50) films were highly transparent, as mentioned before. The morphology of the films prepared at Si/Al = 20 did not change upon the surfactant removal. On the other hand, when the molar Si/Al ratio was 10, the films became rounded tapes with a few mm in width, as shown in Fig. 4c. The SEM image of the film surface for the calcined film prepared at Si/Al = 10 is shown in Fig. 8. Holes with the diameters of some hundreds of nm were ob-

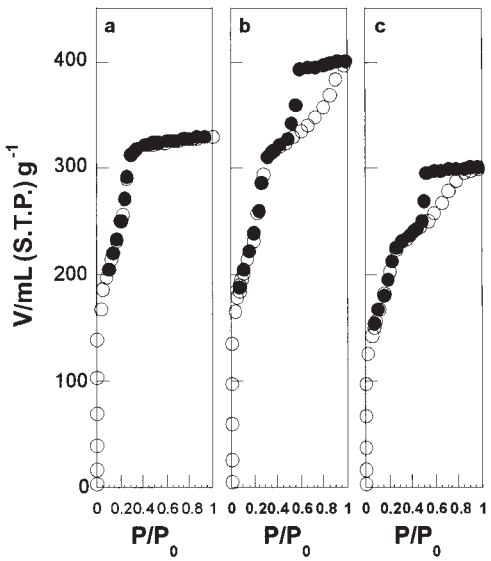

Fig. 6. Nitrogen adsorption/desorption isotherms of the calcined films prepared at Si/C18TAC = 10 and Si/Al = (a) 50, (b) 20, and (c) 10 (adsorption: open circle, desorption: filled circle).

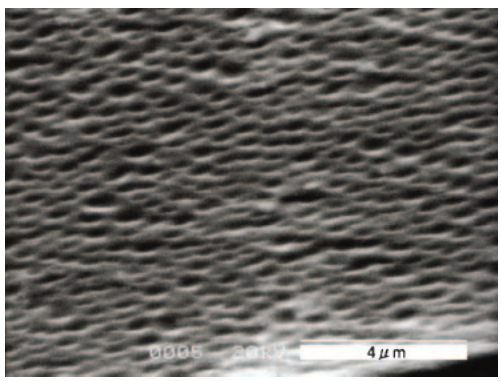

Fig. 8. SEM image of the surface of the calcined film (Si/Al = 10).

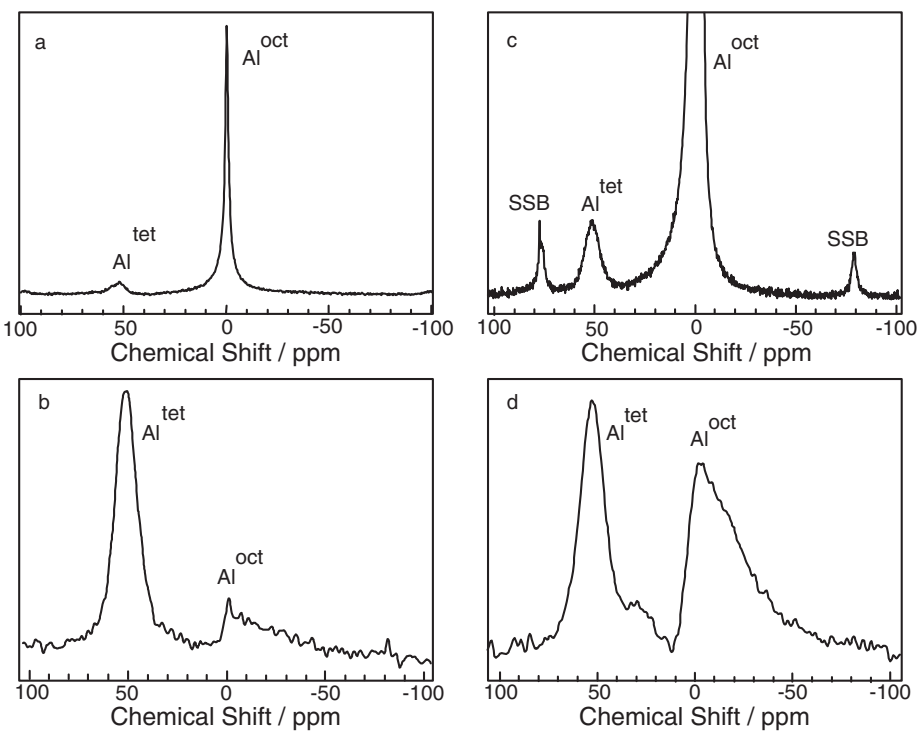

Fig. 7. The ^{27}Al MAS NMR spectra of the aluminum-containing self-standing silica films (a) as-synthesized film (Si/Al = 50), (b) calcined film (Si/Al = 50), (c) as-synthesized film (Si/Al = 20), and (d) calcined film (Si/Al = 20).

served, while the surfaces of the siliceous and low aluminum content (Si/Al = 50) films were smooth, as described before (see Fig. 1 for an example). These holes are thought to scatter light to loose the transparency. The origin of the hole formation is not clear at present.

The ^{27}Al MAS NMR spectra of the film prepared at Si/Al = 20 showed two signals, at 53 and 0 ppm, attributable to tetrahedrally and octahedrally coordinated aluminums, respectively (Figs. 7c and 7d). The relative contribution of the tetrahedrally coordinated aluminum to the octahedrally coordinated one increased to ca. 45% from ca. 5% by the calcination. This result indicated that the heat-treatment promoted the incorporation of aluminum into the silica framework as a result of the chloride anion removal. Similar phenomenon has been reported for the aluminum-containing mesoporous silica powders (Si/Al = 20) prepared with the use of $AlCl_3 \cdot 6H_2O$ as an aluminum source.[43]

The XRD patterns at the surface of the as-synthesized films prepared at Si/Al = 20 (4.8 nm: (200), 4.4 nm: (210), and 4.0 nm: (211)) and 10 (4.6 nm: (200), 4.1 nm: (210), and 3.8 nm: (211)) showed three diffraction peaks ascribable to a cubic (*Pm*3*n*) mesostructure (Figs. 5c and 5e). Sharp diffraction peaks were observed at lower 2θ regions after the calcination, when the molar Si/Al ratio was 20 (Fig. 5d). On the other hand, for the film prepared at Si/Al = 10, the XRD peaks became broad after the calcination (Fig. 5f), suggesting that the regularity of the mesostructures was lost to some extent during the calcination. The XRD patterns at the substrate side of the films prepared at Si/Al = 20 and 10 showed broad peaks similar to those of the films prepared at Si/Al = 50, as described before, indicating a low regularity of the pore arrangement.

Nitrogen adsorption/desorption isotherms for the calcined films prepared at Si/Al = 20 and 10 are shown in Figs. 6b and 6c, respectively. The adsorption isotherms followed type IV, showing that the films were mesoporous. The BET surface areas[41] of the films prepared at Si/Al = 20 and 10 were determined from the adsorption isotherms to be 800 and 740 $m^2\ g^{-1}$, respectively. The average pore diameters were derived from the adsorption isotherms by BJH plots[42] to be 2.6 and 2.4 nm for the films prepared at Si/Al = 20 and 10, respectively. The ^{27}Al MAS NMR spectra and the hysteresis loops in the nitrogen adsorption/desorption isotherms of the calcined films prepared at Si/Al = 20 and 10 suggest the aggregation of the aluminum to cause separation of aluminum oxide particles after the calcination.

Discussion

The siliceous and aluminum-containing (Si/Al = 50, 20, and 10) self-standing mesoporous silica films with a lateral size of a few cm and the thickness of several hundreds of nm were prepared. All the as-synthesized films prepared in the present work possessed ordered mesostructures at the surface. The calcination at 823 K led mesoporous silica films with large BET surface areas over 700 $m^2\ g^{-1}$.

As mentioned in the previous papers on the coating films,[8,39] the solvent evaporation before the gelation is important to obtain highly ordered mesostructures. For the preparation of coating films, highly acidic conditions were employed to obtain highly ordered mesostructures.[8,39] Otherwise, films tend to take less- or no-ordered mesostructures, as a result of the three-dimensional siloxane network formation. The gelation, which directly relates to the formation of the three-dimensional silica network, should be further delayed in the case of the self-standing films, since the solvent evaporation takes a longer time as the film thickness increases. To achieve this requirement, TMVS, which is less reactive than TMOS,[13,15,16] was used as a silica source in our previous paper. In the present system, the rapid gelation was suppressed by mixing the precursor solutions at a low temperature (273 K) as well as by the addition of methanol. Consequently, self-standing films with highly ordered mesostructures and with the thickness of several hundreds of μm, were successfully synthesized.

The mesostructures at the surface and the substrate side of all the as-synthesized films are summarized in Table 3. The mesostructures were governed by the molar Si/C18TAC ratios of the starting solutions. The mesostructures were varied from cubic mesostructures to hexagonal mesostructures with the decrease of the molar Si/hexadecyltrimethylammonium chloride ratios (2.5–8.0) for the coating films.[39] In the present self-standing films, the mesostructures were varied from cubic mesostructures to hexagonal mesostructures with the increase in the molar Si/C18TAC ratios. In the silica-surfactant hybrid systems, silica parts consist of $SiO_2 \cdot nH_2O$ where n is variable. The n values vary depending on the synthetic conditions as a result of the differences in the solvent evaporation rate, so that different sequences on the mesostructure variation were obtained for the coating films and for the present self-standing films.

The pore diameter of the previously reported self-standing porous silica film synthesized from C18TAC, TMOS, and TMVS (the molar TMOS/TMVS ratio of 3) was 1.8 nm,[13] this value was smaller than those of the siliceous films prepared in the present work. Kruk et al. reported that d values, pore diameters, BET surface areas, and pore volumes decreased with the decrease in the tetraethoxysilane/TMVS ratios.[44] The origin of this shrinkage is unclear at present, the absence of TMVS in the present synthesis is worth mentioning as a merit for the pore size tuning.

Table 3. The Mesostructures of the Siliceous and the Aluminum-Containing Self-Standing Mesoporous Silica Films at Various the Molar Si/C18TAC and the Si/Al Ratios

	Si/C18TAC = 8	Si/C18TAC = 9	Si/C18TAC = 10	Si/C18TAC = 11
Al/Si = 0	C/H	H/H	H/H	H/H
Al/Si = 1/50		C/D	H/D	H/D
Al/Si = 1/20			C/D	
Al/Si = 1/10			C/D	

Letters denote the observed mesostructures (the surface/the substrate side); C: cubic, H: hexagonal, and D: disordered.

The aluminum-containing self-standing mesoporous silica films with the thickness of ca. 50 μm, were successfully prepared. The use of aluminum tri(*sec*-butoxide) as an aluminum source of the self-standing films may result in the rapid gelation and the generation of aluminum oxide particles, because aluminum tri(*sec*-butoxide) was highly reactive to water. To avoid this problem, we used $AlCl_3 \cdot 6H_2O$ as the aluminum source. The precursor solution at Si/Al = 10 became turbid by stirring for ca. 30 min, suggesting the generation of aluminum-containing silica particles. The added aluminum was incorporated into the silica walls as tetrahedrally coordinated species during the heat-treatment for the surfactant removal. After the calcination, ca. 85 and ca. 45% of aluminums were present as tetrahedrally coordinated species in the films prepared at Si/Al = 50 and 20, respectively. Thus, the relative contributions of tetrahedrally coordinated aluminum to silicon were ca. 60 and ca. 45% for the films prepared at Si/Al = 50 and 20, respectively, suggesting that the silica walls had the limitations of the incorporated aluminum amount.

Table 3 indicates that the mesostructures were also governed by the amount of aluminum added. For example, in the case of the films prepared at Si/C18TAC = 9, the mesostructures at the surface of the siliceous and aluminum-containing (Si/Al = 50) films were a hexagonal and a cubic mesostructure, respectively. The aluminum-containing films did not possess ordered mesostructures at the substrate side, irrespective of the Si/C18TAC and the Si/Al ratios. The reason for this is not clear at present.

The BET surface areas and the pore diameters became smaller with the increase in the aluminum content. Similar phenomena have been observed for the aluminum-containing mesoporous silica powders.[38,43,45] The nitrogen adsorption/desorption isotherms of the films prepared at Si/Al = 20 and 10 showed hysteresis loops at P/P_0 values between 0.45 and 1.0 (Figs. 6b and 6c), while the siliceous and the low aluminum content (Si/Al = 50) films did not show hysteresis loops (Figs. 3 and 6a). The observed hysteresis loops were not due to the capillary condensation because the average pore diameters of the calcined films (2.4–2.6 nm) were not large enough to exhibit a hysteresis loop.[46] Lin et al. pointed out that such a hysteresis loop indicated the formation of some structural defects in the mesostructure.[47] We thought that the existence of aluminum oxide particles in the pore caused the hysteresis loops of the films prepared at Si/Al = 20 and 10.

As to the aluminum-containing mesoporous silica powders, it has been reported that almost all the aluminum was incorporated into the silica walls when the molar Si/Al ratios were over ca. 40.[28,47] The ^{27}Al MAS NMR spectra and the nitrogen adsorption/desorption isotherms of the present aluminum-containing films suggest that almost all the added aluminum was incorporated into the silica walls when the molar Si/Al ratio of the film was 50. The present results are consistent with these observations. On the other hand, there have been several attempts to increase aluminum content, probably for the purpose of increasing the population of acidic sites on the mesopore. Ryoo et al. synthesized aluminum-containing mesoporous silica powders, whose ^{27}Al MAS NMR spectra showed a single peak attributable to tetrahedrally coordinated aluminum, at the molar Si/Al ratios of 5, 15, and 30 with the use of sodium aluminate as the aluminum source.[26] The sodium aluminate was added to the mixture after heating at 370 K which was synthesized from sodium silicate, ammonia aqueous solution, and hexadecyltrimethylammonium chloride. The mixture was heated again at 370 K to prepare the aluminum-containing silica-surfactant powders.[26] Aluminum-containing mesoporous silica powders (molar Si/Al ratios were over 5) with large tetrahedral coordinated aluminum content were also prepared by a grafting method which consisted of reacting the silanol groups present in siliceous mesoporous silica powder with discrete amounts of aluminum alkoxide, followed by calcination to anchor the aluminum.[48] These strategies seem to be difficult to apply for the films, however, the attempts are worth conducting. Further variation of aluminum content and other evaluation of the effects of the incorporated aluminum on the surface properties are being made in our laboratory.

Conclusion

The siliceous and aluminum-containing self-standing mesoporous silica films (with the molar Si/Al ratios of 50, 20, and 10) were synthesized by the solvent evaporation method from tetramethoxysilane, aluminum chloride hexahydrate, and octadecyltrimethylammonium chloride. The siliceous and aluminum-containing films prepared at Si/Al = 50 were transparent, and the aluminum-containing films prepared at Si/Al = 20 and 10 were cloudy. The films possessed highly ordered mesostructures and large surface areas (over ca. 700 $m^2\ g^{-1}$). The mesostructures of the products were affected by the molar ratios of the Si/C18TAC and the Si/Al. Aluminum was incorporated as tetrahedrally coordinated species in the silica framework at the molar Si/Al ratio of 50. Addition of greater amounts of aluminum resulted in the formation of aluminum oxide particles, probably in the mesopore.

This work was supported by a Grant-in-Aid for Scientific Research on Priority Areas (417) from the Ministry of Education, Culture, Sports, Science and Technology (MEXT).

References

1 K. Moller and T. Bein, *Chem. Mater.*, **10**, 2950 (1998).
2 A. Stein, B. J. Melde, and R. C. Schroden, *Adv. Mater.*, **12**, 1403 (2000).
3 A. Sayari and S. Hamoudi, *Chem. Mater.*, **13**, 3151 (2001).
4 M. Ogawa, *J. Photochem. Photobiol., C*, **3**, 129 (2002).
5 S. Mann and G. A. Ozin, *Nature*, **382**, 313 (1996).
6 M. Ogawa, *Curr. Top. Colloid Interface Sci.*, **4**, 209 (2001).
7 M. Ogawa, *J. Am. Chem. Soc.*, **116**, 7941 (1994).
8 M. Ogawa, *Chem. Commun.*, **1996**, 1149.
9 T. Dabadie, A. Ayral, C. Guizard, L. Cot, and P. Lacan, *J. Mater. Chem.*, **6**, 1789 (1996).
10 J. E. Martin, M. T. Anderson, J. Odinek, and P. Newcomer, *Langmuir*, **13**, 4133 (1997).
11 A. Sellinger, P. M. Weiss, A. Nguyen, Y. Lu, R. A. Assink, W. Gong, and C. J. Brinker, *Nature*, **394**, 256 (1998).
12 Y. Lu, R. Ganguli, C. A. Drewien, M. T. Anderson, C. J. Brinker, W. Gong, Y. Guo, H. Soyez, B. Dunn, M. H. Huang, and J. I. Zink, *Nature*, **389**, 364 (1997).
13 M. Ogawa and T. Kikuchi, *Adv. Mater.*, **10**, 1077 (1998).
14 R. Ryoo, C. H. Ko, S. J. Cho, and J. M. Kim, *J. Phys. Chem. B*, **101**, 10610 (1997).

15 M. Ogawa, K. Ikeue, and M. Anpo, *Chem. Mater.*, **13**, 2900 (2001).
16 K. Ikeue, S. Nozaki, M. Ogawa, and M. Anpo, *Catal. Lett.*, **80**, 111 (2002).
17 P. J. Bruinsma, A. Y. Kim, J. Liu, and S. Baskaran, *Chem. Mater.*, **9**, 2507 (1997).
18 M. Ogawa and N. Yamamoto, *Langmuir*, **15**, 2227 (1999).
19 D. Zhao, P. Yang, N. Melosh, J. Feng, B. F. Chmelka, and G. D. Stucky, *Adv. Mater.*, **10**, 1380 (1998).
20 N. A. Melosh, P. Davidson, P. Feng, D. J. Pine, and B. F. Chmelka, *J. Am. Chem. Soc.*, **123**, 1240 (2001).
21 Y. Lu, H. Fan, N. Doke, D. A. Loy, R. A. Assink, D. A. L. Van, and C. J. Brinker, *J. Am. Chem. Soc.*, **122**, 5258 (2000).
22 A. Stein and B. Holland, *J. Porous Mater.*, **3**, 83 (1996).
23 A. Tuel, *Microporous Mesoporous Mater.*, **27**, 151 (1999).
24 J. S. Beck, J. C. Vartuli, W. L. Roth, M. E. Leonowics, C. T. Kresge, K. D. Schmitt, C. T.-W. Chu, D. H. Olson, E. W. Sheppard, S. B. McCullen, J. B. Higgins, and J. L. Schlenker, *J. Am. Chem. Soc.*, **114**, 10834 (1992).
25 R. Mokaya, *Adv. Mater.*, **12**, 1681 (2000).
26 R. Ryoo, C. H. Ko, and R. F. Howe, *Chem. Mater.*, **9**, 1607 (1997).
27 Z. Luan, C.-F. Cheng, H. He, and J. Klinowski, *J. Phys. Chem.*, **99**, 10590 (1995).
28 J. Weglarski, J. Datka, H. He, and J. Klinowski, *J. Chem. Soc., Faraday Trans.*, **92**, 5161 (1996).
29 P. T. Tanev, M. Chibwe, and T. J. Pinnavaia, *Nature*, **368**, 321 (1994).
30 W. Zhang, M. Fröba, J. Wang, P. T. Tanev, J. Wong, and T. J. Pinnavaia, *J. Am. Chem. Soc.*, **118**, 9164 (1996).
31 T. Maschmeyer, F. Rey, G. Sankar, and J. M. Thomas, *Nature*, **378**, 159 (1995).
32 J. V. Walker, M. Morey, H. Carlsson, A. Davidson, G. D. Stucky, and A. Butler, *J. Am. Chem. Soc.*, **119**, 6921 (1997).
33 H. M. Sung-Suh, Z. Luan, and L. Kevan, *J. Phys. Chem. B*, **101**, 10455 (1997).
34 K. Ikeue, H. Yamashita, and M. Anpo, *Chem. Lett.*, **1999**, 1135.
35 S. G. Zhang, Y. Fujii, H. Yamashita, K. Koyano, T. Tatsumi, and M. Anpo, *Chem. Lett.*, **1997**, 659.
36 A. Corma, H. García, M. T. Navarro, E. J. Palomares, and F. Rey, *Chem. Mater.*, **12**, 3068 (2000).
37 M. Ogawa, K. Kuroda, and J. Mori, *Chem. Commun.*, **2000**, 2441.
38 M. Ogawa, K. Kuroda, and J. Mori, *Langmuir*, **18**, 744 (2002).
39 M. Ogawa and N. Masukawa, *Microporous Mesoporous Mater.*, **38**, 35 (2000).
40 S. Besson, T. Gacoin, C. Jacquiod, C. Ricolleau, D. Babonneau, and J.-P. Boilot, *J. Mater. Chem.*, **10**, 1331 (2000).
41 S. Brunauer, P. H. Emmett, and E. Teller, *J. Am. Chem. Soc.*, **60**, 309 (1938).
42 E. P. Barrett, L. G. Joyner, and P. P. Halenda, *J. Am. Chem. Soc.*, **73**, 373 (1951).
43 Z. Luan, M. Hartmann, D. Zhao, W. Zhou, and L. Kevan, *Chem. Mater.*, **11**, 1621 (1999).
44 M. Kruk, T. Asefa, M. Jaroniec, and G. A. Ozin, *J. Am. Chem. Soc.*, **124**, 6383 (2002).
45 R. Mokaya and W. Jones, *Chem. Commun.*, **1996**, 981.
46 S. Inoue, Y. Hanzawa, and K. Kaneko, *Langmuir*, **14**, 3079 (1998).
47 H.-P. Lin, S.-T. Wong, C.-Y. Mou, and C.-Y. Tang, *J. Phys. Chem. B*, **104**, 8967 (2000).
48 R. Mokaya and W. Jones, *Chem. Commun.*, **1997**, 2185.